

Dynamic multiscaling in magnetohydrodynamic turbulence*

Samriddhi Sankar Ray,^{1,†} Ganapati Sahoo,^{2,‡} and Rahul Pandit^{3,§}

¹*International Centre for Theoretical Sciences, Tata Institute of Fundamental Research, Bangalore 560089, India.*

²*Department of Physics and INFN, University of Rome “Tor Vergata”, Via della Ricerca Scientifica 1, 00133, Rome, Italy.*

³*Centre for Condensed Matter Theory, Department of Physics, Indian Institute of Science, Bangalore 560012, India.*

We present the first study of the multiscaling of time-dependent velocity and magnetic-field structure functions in homogeneous, isotropic magnetohydrodynamic (MHD) turbulence in three dimensions. We generalize the formalism that has been developed for analogous studies of time-dependent structure functions in fluid turbulence to MHD. By carrying out detailed numerical studies of such time-dependent structure functions in a shell model for three-dimensional MHD turbulence, we obtain both equal-time and dynamic scaling exponents.

PACS numbers: 47.27.Gs, 47.65.-d, 52.65.Kj, 05.45.-a

I. INTRODUCTION

Velocity and magnetic-field structure functions, which are moments of the probability distribution function (PDF) of the differences of fluid velocities and magnetic fields between two points separated by a distance r (a precise definition is given below), are often used to characterize the statistical properties of homogeneous, isotropic magnetohydrodynamic (MHD) turbulence [1, 2]. If r is in the *inertial range* of scales that lie between the large length scale L , at which energy is pumped into the system, and the fluid and magnetic dissipation scales η_d^u and η_d^b , respectively, at which dissipation becomes significant, these structure functions scale as a power of r . This is similar to the power-law behaviors of correlation functions at a critical point in, say, a spin system, as has been elucidated for *equal-time* structure functions in many papers: It turns out that the simple scaling we see at most critical points must be generalized to multiscaling in turbulence; i.e., an infinity of exponents is required to characterize the inertial-range behaviors of structure functions of different orders as discussed, e.g., for fluid turbulence in Ref. [3] and for three-dimensional (3D) MHD turbulence in Ref. [1].

The scaling behaviors of correlation functions at a critical point [4] arise from the divergence of a correlation length $\bar{\xi}$ at the critical point: in a simple spin system $\bar{\xi} \sim \bar{t}^{-\nu}$ if the magnetic field $H = 0$, where the reduced temperature $\bar{t} \equiv (T - T_c)/T_c$, T is the temperature, T_c the critical temperature, and ν is an equal-time critical exponent that is universal (in a given universality class). In the vicinity of a critical point the relaxation time τ , which follows from *time-dependent* correlation functions,

scales, according to the *dynamic-scaling Ansatz*, as

$$\tau \sim \bar{\xi}^z; \quad (1)$$

z is known as the dynamic-scaling exponent. There has been considerable progress [5–14] in developing the analog of such a dynamic-scaling *Ansatz* for *time-dependent* structure functions in homogeneous, isotropic fluid turbulence. In this paper we present the first study of time-dependent structure functions in MHD turbulence. We first set up the formalism in the framework of the 3D MHD equations and then carry out explicit numerical studies of a shell model for 3D MHD turbulence [2]. We show that (a) an infinity of dynamic-multiscaling exponents is required and (b) that these exponents depend on the precise way in which times, e.g., the integral-time scales (defined below), are extracted from time-dependent structure functions.

Since the work of Obukhov [15], Desnyansky and Novikov [16], and Gledzer, and Ohkitani and Yamada [17, 18] (GOY), shell models have been used to study the multiscaling of velocity structure functions in fluid turbulence [3, 19–26]. Generalizations of these models have been used to study magnetohydrodynamic (MHD) turbulence [2, 27–31], Hall-MHD turbulence [32–35], the effects of polymer additives on fluid turbulence [36], two-dimensional fluid turbulence [37] and turbulence in between two and three dimensions [38], turbulence in rotating systems [39] and in binary-fluid mixtures [40], superfluid turbulence [41–44], and the dynamic multiscaling of time-dependent structure functions in fluid [6, 12, 13] and passive-scalar [7] turbulence. It behooves us, therefore, to examine first the dynamic multiscaling of structure functions in a shell model for three-dimensional MHD (3D MHD).

In fluid and passive-scalar turbulence, dynamic-multiscaling exponents are related by *linear bridge relations* to equal-time multiscaling exponents [7, 12–14]; we have not been able to find such relations for MHD turbulence so far. Therefore, we obtain equal-time and time-dependent structure functions for a shell model for 3D MHD turbulence and, from these, equal-time and dy-

*Postprint version of the manuscript published in Phys. Rev. E **94**, 053101 (2016)

[†]Electronic address: samriddhisankararray@gmail.com

[‡]Electronic address: ganapati.sahoo@gmail.com

[§]Electronic address: rahul@physics.iisc.ernet.in

dynamic multiscaling exponents. We then try to see if these suggest any bridge relations.

The remaining part of this paper is organized as follows: Section II contains an introduction to the 3D MHD equations and the multiscaling of equal-time magnetic and fluid structure functions. Section III is devoted to a discussion of the dynamic multiscaling of time-dependent structure functions in fluid turbulence, in general, and 3D MHD turbulence, in particular. In Section IV we describe a shell model for 3D MHD turbulence and give the details of our numerical studies of this model. Section V presents results from our simulations for time-dependent structure functions; and in Section VI we make some concluding remarks.

II. MAGNETOHYDRODYNAMICS AND MULTISCALING

The flow of conducting fluids can be described by the following 3D MHD equations [45] for the velocity field $\mathbf{u}(\mathbf{x}, t)$ and the magnetic field $\mathbf{b}(\mathbf{x}, t)$ at point \mathbf{x} and time t :

$$\frac{\partial \mathbf{u}}{\partial t} + (\mathbf{u} \cdot \nabla) \mathbf{u} = \nu \nabla^2 \mathbf{u} - \nabla \bar{p} + \frac{1}{4\pi} (\mathbf{b} \cdot \nabla) \mathbf{b} + \mathbf{f}_u; \quad (2)$$

$$\frac{\partial \mathbf{b}}{\partial t} = \nabla \times (\mathbf{u} \times \mathbf{b}) + \eta \nabla^2 \mathbf{b} + \mathbf{f}_b; \quad (3)$$

here ν and η are the kinematic viscosity and the magnetic diffusivity, respectively, and the effective pressure $\bar{p} = p + (b^2/8\pi)$, where p is the pressure; \mathbf{u} and \mathbf{b} have the same dimensions in this formalism [45]. For low-Mach-number flows, to which we restrict ourselves, we use the incompressibility condition $\nabla \cdot \mathbf{u} = 0$, which we use, along with the constraint $\nabla \cdot \mathbf{b} = 0$, to eliminate the pressure \bar{p} in Eq. (2). We choose a uniform density $\rho = 1$ and the external forces \mathbf{f}_u and \mathbf{f}_b inject energy into the conducting fluid, typically at large length scales. In decaying turbulence, the external forces are absent. The dimensionless parameters that characterize 3D MHD turbulence are the kinetic Reynolds number $\text{Re} \equiv (\ell v)/\nu$, the magnetic Reynolds number $\text{Re}_M \equiv (\ell v)/\eta$, and the magnetic Prandtl number $\text{Pr}_M \equiv \text{Re}_M/\text{Re} = \nu/\eta$; here ℓ and v are the characteristic length and velocity scales of the flow.

It is useful to characterize the statistical properties of MHD turbulence through the order- p , equal-time, structure functions of the longitudinal component of increments of the velocity field, $\delta u_{\parallel}(\mathbf{x}, \mathbf{r}, t) \equiv [\mathbf{u}(\mathbf{x} + \mathbf{r}, t) - \mathbf{u}(\mathbf{x}, t)] \cdot \mathbf{r}/r$, and the magnetic field, $\delta b_{\parallel}(\mathbf{x}, \mathbf{r}, t) \equiv [\mathbf{b}(\mathbf{x} + \mathbf{r}, t) - \mathbf{b}(\mathbf{x}, t)] \cdot \mathbf{r}/r$. These structure functions are

$$\mathcal{S}_p^u(r) \equiv \langle [\delta u_{\parallel}(\mathbf{x}, \mathbf{r}, t)]^p \rangle \sim r^{\zeta_p^u}; \quad (4)$$

$$\mathcal{S}_p^b(r) \equiv \langle [\delta b_{\parallel}(\mathbf{x}, \mathbf{r}, t)]^p \rangle \sim r^{\zeta_p^b}; \quad (5)$$

they show power-law dependences on r for the inertial range $\eta_d^u, \eta_d^b \ll r \ll L$. The angular brackets denote an average over the statistically steady state of forced

3D MHD turbulence or an average over different initial configurations for decaying 3D MHD turbulence.

In contrast with the scaling behaviors of correlation functions at conventional critical points in equilibrium statistical mechanics, in 3D MHD turbulence the structure functions $\mathcal{S}_p^u(r)$ and $\mathcal{S}_p^b(r)$ do not exhibit simple scaling forms: numerical evidence suggests that these structure functions exhibit multiscaling, with ζ_p^u and ζ_p^b nonlinear, convex, monotonically increasing functions of p [1, 46]. In the absence of a mean magnetic field, an extension of the 1941 phenomenological theory of Kolmogorov (K41) [47] yields simple scaling with $\zeta_p^{u,K41} = \zeta_p^{b,K41} = p/3$; but the measured values of ζ_p^u and ζ_p^b , e.g., deviate significantly from the K41 prediction, especially for $p > 3$ (see, e.g., Ref. [1]). Even though the K41 phenomenology fails to capture the multiscaling of the equal-time structure function $\mathcal{S}_p(r)$, it provides us with important conceptual underpinnings for studies of homogeneous, isotropic 3D MHD turbulence in the absence of a mean magnetic field. In the presence of a mean magnetic field, Alfvén waves are present; they introduce a new time scale into the problem, so Iroshnikov [48], Kraichnan [49], and Dobrowlny, *et al.* [50] have suggested that the energy spectrum $E(k)$ can scale as $k^{-3/2}$, rather than $k^{-5/3}$, which follows from the K41 phenomenology. We refer the reader to Refs. [45, 51] for a discussion of the Dobrowlny-Iroshnikov-Kraichnan phenomenology. We restrict ourselves to the case when the mean magnetic field vanishes.

Several recent studies, especially on solar-wind data, have yielded equal-time, two-point correlations that are consistent with the phenomenological picture we have described above [52]. Shell models, of the type we use here, have played a key role in understanding such correlations and emphasizing, e.g., the importance of the Hall term in astrophysical MHD (see the elucidation of the dual spectral scaling ranges, seen in solar-wind data, in the careful shell-model investigations of Refs. [32–35]). In the coming years, advances in probes for the solar wind and interplanetary plasmas should lead to accurate measurements of not only spatial correlations but also of spatiotemporal correlations of the turbulent fields in these systems; it is in this light that our study, which characterizes such spatiotemporal correlations in MHD turbulence and unearths their multiscaling nature, assumes special importance.

III. DYNAMIC MULTISCALING

To set the stage for our discussions on time-dependent structure functions in MHD turbulence, it is useful first to recall the results of analogous studies in fluid turbulence.

A naïve generalisation of K41 phenomenology to time-dependent velocity structure functions in fluid turbulence yields simple dynamic scaling with a dynamic exponent $z_p^{K41} = 2/3$ for all orders p . In order to obtain non-trivial

Pr_M	ν	η	u_{rms}	b_{rms}	λ	$\text{Re}_{\lambda,u}$	$\text{Re}_{\lambda,b}$	τ_u	τ_b
0.1	10^{-7}	10^{-6}	0.84	1.27	0.879	7425500	742550	7.24	15.70
1.0	5×10^{-7}	5×10^{-7}	0.85	1.27	0.955	1625465	1625465	7.09	15.71
10.0	10^{-6}	10^{-7}	0.83	1.28	0.873	724918	7249184	7.41	15.72

TABLE I: Parameters for our simulations of decaying 3D MHD turbulence for the three Prandtl numbers. These parameters are defined in the text.

dynamic exponents, we need time-dependent velocity structure functions and we must distinguish between Eulerian (\mathcal{E}), Lagrangian (\mathcal{L}), and quasi-Lagrangian (QL) fields. Eulerian fields yield trivial dynamic scaling with $z^{\mathcal{E}} = 1$, for all p , because of the sweeping effect and, hence, nontrivial dynamic multiscaling is possible only for Lagrangian [53] or quasi-Lagrangian [8] velocity structure functions. The latter are defined in terms of the quasi-Lagrangian velocity $\hat{\mathbf{u}}$ that is related to its Eulerian counterpart \mathbf{u} as follows:

$$\hat{\mathbf{u}}(\mathbf{x}, t) \equiv \mathbf{u}[\mathbf{x} + \mathbf{R}(t; \mathbf{r}_0, 0), t], \quad (6)$$

with $\mathbf{R}(t; \mathbf{r}_0, 0)$ the position at time t of a Lagrangian particle that was at \mathbf{r}_0 at time $t = 0$. Equal-time, quasi-Lagrangian velocity structure functions are the same as their Eulerian counterparts [14, 54].

For MHD turbulence we can define the order- p , time-dependent, structure functions, for longitudinal, quasi-Lagrangian velocity and magnetic-field increments as follows:

$$\mathcal{F}_p^u(r, \{t_1, \dots, t_p\}) \equiv \langle [\delta \hat{u}_{\parallel}(\mathbf{x}, t_1, r) \dots \delta \hat{u}_{\parallel}(\mathbf{x}, t_p, r)] \rangle; \quad (7)$$

$$\mathcal{F}_p^b(r, \{t_1, \dots, t_p\}) \equiv \langle [\delta \hat{b}_{\parallel}(\mathbf{x}, t_1, r) \dots \delta \hat{b}_{\parallel}(\mathbf{x}, t_p, r)] \rangle. \quad (8)$$

(See Refs. [12–14] for similar structure functions for fluid and passive-scalar turbulence.) In our studies of scaling properties, we restrict r to lie in the inertial range and consider, for simplicity, $t_1 = t$ and $t_2 = \dots = t_p = 0$ and denote the structure functions, defined in Eqs. (7) and (8), by $\mathcal{F}_p^u(r, t)$ and $\mathcal{F}_p^b(r, t)$, respectively. Given $\mathcal{F}_p^u(r, t)$ and $\mathcal{F}_p^b(r, t)$, there are different ways of extracting time scales. For example, we can define order- p , degree- M integral-time scale (superscript I) for the velocity field as follows:

$$\mathcal{T}_{p,M}^{I,u}(r) \equiv \left[\frac{1}{\mathcal{S}_p^u(r)} \int_0^\infty \mathcal{F}_p^u(r, t) t^{(M-1)} dt \right]^{(1/M)}; \quad (9)$$

their analog for the magnetic field is

$$\mathcal{T}_{p,M}^{I,b}(r) \equiv \left[\frac{1}{\mathcal{S}_p^b(r)} \int_0^\infty \mathcal{F}_p^b(r, t) t^{(M-1)} dt \right]^{(1/M)}. \quad (10)$$

If the integrals in Eqs. (9) and (10) exist, we can generalize the dynamic-scaling *Ansatz* (1) at a critical point to the following dynamic-multiscaling *Ansätze* for homogeneous, isotropic MHD turbulence [for fluid turbulence see Refs. [12–14]]. For the velocity integral-time scales we assume

$$\mathcal{T}_{p,M}^{I,u}(r) \sim r^{z_{p,M}^{I,u}}; \quad (11)$$

and, similarly, for the magnetic integral-time scales

$$\mathcal{T}_{p,M}^{I,b}(r) \sim r^{z_{p,M}^{I,b}}. \quad (12)$$

These equations define, respectively, the integral-time dynamic-multiscaling exponents $z_{p,M}^{I,u}$ and $z_{p,M}^{I,b}$. Time scales based on derivatives can be defined as in Refs. [12–14]. For the purpose of illustrating dynamic multiscaling of structure functions in 3D MHD turbulence, it suffices to use integral time scales, to which we restrict ourselves in the remaining part of this paper. We return to the issue of other time-scales, e.g., the derivative time-scale in the concluding section of this paper.

IV. THE 3D MHD SHELL MODEL

We carry out extensive numerical simulations to obtain equal-time and dynamic multiscaling exponents for a GOY-type [3, 17, 18] shell model for three-dimensional MHD turbulence [2]. This shell model is defined on a logarithmically discretized Fourier space labelled by scalar wave vectors k_n that are associated with the shells n . The dynamical variables are the complex scalar shell velocities u_n and magnetic fields b_n . The evolution equations for u_n and b_n for 3D MHD are given by

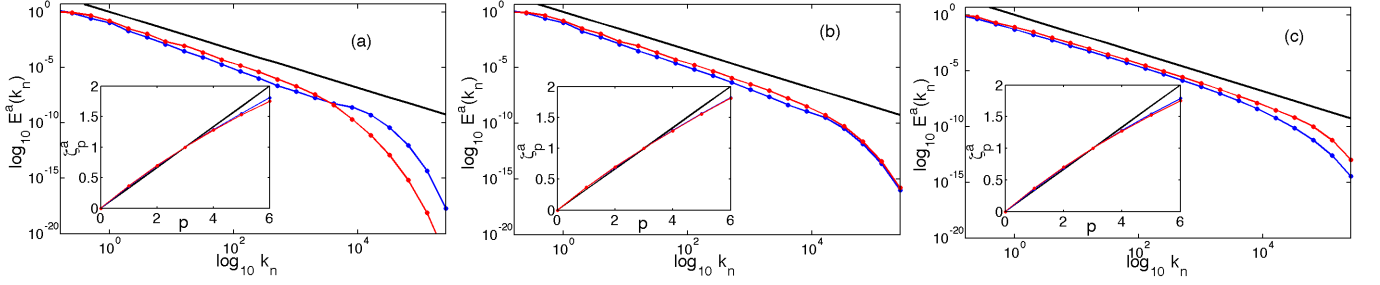


FIG. 1: (Color online) Log-log plots of the fluid kinetic (blue, filled circles) and magnetic (red, filled squares) energy spectra versus the wave-vector for (a) $\text{Pr}_M = 0.1$, (b) $\text{Pr}_M = 1.0$, and (c) $\text{Pr}_M = 10.0$. The black line is the K41 line that indicates $k^{-5/3}$ scaling. Insets : Plots of the equal-time scaling-exponent ratios ζ_p^u/ζ_3^u (blue, filled circles) and ζ_p^b/ζ_3^b (red, filled squares), for the fluid and magnetic equal-time structure functions, respectively, versus the order p , for the same values of the Prandtl Number Pr_M ; the black line denotes the K41 line $p/3$, which is shown for reference. Note: The negative values on the vertical axes are a result the logarithmic scales we use.

$$\frac{du_n}{dt} + \nu k_n^2 u_n = \iota [A_n(u_{n+1}u_{n+2} - b_{n+1}b_{n+2}) + B_n(u_{n-1}u_{n+1} - b_{n-1}b_{n+1}) + C_n(u_{n-2}u_{n-1} - b_{n-2}b_{n-1})]^*; \quad (13)$$

$$\frac{db_n}{dt} + \eta k_n^2 b_n = \iota [D_n(u_{n+1}b_{n+2} - b_{n+1}u_{n+2}) + E_n(u_{n-1}b_{n+1} - b_{n-1}u_{n+1}) + F_n(u_{n-2}b_{n-1} - b_{n-2}u_{n-1})]^*; \quad (14)$$

here $k_n = k_0 2^n$, $k_0 = 1/16$, complex conjugation is denoted by $*$, and the coefficients

$$A_n = k_n, \quad B_n = -k_{n-1}/2, \quad C_n = -k_{n-2}/2, \quad D_n = k_n/6, \quad E_n = k_{n-1}/3, \quad F_n = -2k_{n-2}/3, \quad (15)$$

are chosen to conserve the shell-model analogs of the total energy $E_T = E_u + E_b \equiv (1/2) \sum_n (|u_n|^2 + |b_n|^2)$, cross helicity $H_C \equiv (1/2) \sum_n (u_n b_n^* + u_n^* b_n)$, and magnetic helicity $H_M \equiv \sum_n (-1)^n |b_n|^2 / k_n$, in the inviscid, unforced limit, and $1 \leq n \leq N$. The logarithmic discretization of Fourier space allows us to reach very high Reynolds numbers in numerical simulations of this shell model even with $N = 22$.

The shell-model equations allow for direct interactions only between nearest- and next-nearest-neighbor shells. By contrast, in the Fourier transform of the 3D MHD equations, every Fourier mode of the velocity and magnetic fields is coupled to every other Fourier mode directly. This leads to direct sweeping of small eddies by large ones and to the trivial dynamic scaling of Eulerian velocity structure functions that we have mentioned above. Our shell model does not have direct sweeping in this sense; thus, such shell models are sometimes thought of as simplified, quasi-Lagrangian versions of their parent hydrodynamic equations. Therefore, we expect nontrivial dynamic multiscaling for structure functions in this

MHD shell model as has been found [12, 13] for the GOY model for fluid turbulence.

The equal-time, velocity and magnetic field structure functions, in the MHD shell model, are defined as

$$S_p^u(k_n) \equiv \langle [u_n(t) u_n^*(t)]^{p/2} \rangle \quad (16)$$

and

$$S_p^b(k_n) \equiv \langle [b_n(t) b_n^*(t)]^{p/2} \rangle, \quad (17)$$

respectively. For shells lying in the inertial range, we obtain the equal-time scaling exponents via $S_p^u(k_n) \sim k_n^{-\zeta_p^u}$ and $S_p^b(k_n) \sim k_n^{-\zeta_p^b}$. The three cycles [55] in the static solutions of shell models lead to rough, period-three oscillations in $S_p^u(k_n)$ and $S_p^b(k_n)$. Hence, in order to obtain scaling regions without such oscillations, we generalize the modified structure functions suggested in Ref. [55] for the GOY model for our MHD shell model.

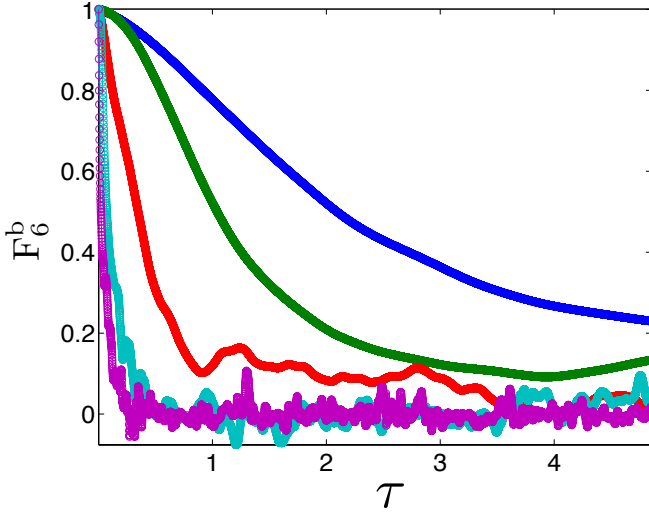


FIG. 2: (Color online) A representative plot of the normalised, time-dependent sixth-order structure function F_6^b , for the magnetic field, versus the normalised time $\tau = t/\tau_b$, where τ_b is the characteristic small time-scale associated with the magnetic field. The different curves correspond to shell numbers 5 (uppermost, in blue), 6, 9, 12, and 15 (lowermost, in magenta). The plot is shown for $\text{Pr}_M = 1.0$.

In particular, we use

$$\begin{aligned} \Sigma_p^u &\equiv \left\langle |\Im[u_{n+2}u_{n+1}u_n - (1/4)u_{n-1}u_nu_{n+1}]|^{p/3} \right\rangle, \\ \Sigma_p^b &\equiv \left\langle |\Im[b_{n+2}b_{n+1}b_n - (1/4)b_{n-1}b_nb_{n+1}]|^{p/3} \right\rangle; \end{aligned} \quad (18)$$

in these structure functions, the period-three oscillations are effectively filtered out. We can also obtain the exponent ratios ζ_p^u/ζ_3^u and ζ_p^b/ζ_3^b by using the extended-self-similarity (ESS) procedure in which we plot, respectively, S_p^u versus S_3^u and S_p^b versus S_3^b (see, e.g., Refs. [1, 56]).

We then employ the order- p , time-dependent structure functions for the 3D MHD shell model, namely,

$$F_p^u(k_n, t_0, t) \equiv \left\langle [u_n(t_0)u_n^*(t_0 + t)]^{p/2} \right\rangle; \quad (19)$$

$$F_p^b(k_n, t_0, t) \equiv \left\langle [b_n(t_0)b_n^*(t_0 + t)]^{p/2} \right\rangle, \quad (20)$$

to obtain the integral time scales. In general, these time-dependent structure functions are complex; we find that their imaginary parts are much smaller than their real parts; therefore, in all our studies, we restrict ourselves to the real parts of these time-dependent structure functions. References [6, 7, 12–14] have used such time-dependent structure functions to verify bridge relations for fluid and passive-scalar turbulence. Both equal-time and time-dependent structure functions can also be obtained for the shell-model analogs of the Elsässer variables $z_n^\pm = u_n \pm b_n$.

The root-mean-square velocity and the root-mean-square magnetic field are defined, respectively, as $u_{\text{rms}} =$

p	ζ_p^u (ESS)	ζ_p^b (ESS)	$z_{p,1}^{I,u}$	$z_{p,1}^{I,b}$
1	0.362 ± 0.005	0.367 ± 0.004	0.593 ± 0.001	0.597 ± 0.001
2	0.694 ± 0.004	0.698 ± 0.004	0.622 ± 0.004	0.632 ± 0.002
3	1.0000	1.0000	0.623 ± 0.007	0.629 ± 0.003
4	1.287 ± 0.008	1.277 ± 0.006	0.62 ± 0.01	0.627 ± 0.007
5	1.548 ± 0.009	1.528 ± 0.009	0.62 ± 0.01	0.629 ± 0.009
6	1.81 ± 0.03	1.75 ± 0.03	0.61 ± 0.02	0.63 ± 0.01

TABLE II: The equal-time (ESS) and the integral-time dynamic multiscaling exponents for the fluid and the magnetic field from our simulations of decaying MHD turbulence for the magnetic Prandtl Number $\text{Pr}_M = 0.1$.

p	ζ_p^u (ESS)	ζ_p^b (ESS)	$z_{p,1}^{I,u}$	$z_{p,1}^{I,b}$
1	0.361 ± 0.003	0.367 ± 0.003	0.616 ± 0.005	0.618 ± 0.002
2	0.692 ± 0.004	0.696 ± 0.003	0.641 ± 0.003	0.646 ± 0.002
3	1.0000	1.0000	0.645 ± 0.004	0.641 ± 0.002
4	1.288 ± 0.007	1.284 ± 0.006	0.643 ± 0.006	0.634 ± 0.003
5	1.564 ± 0.009	1.554 ± 0.009	0.639 ± 0.007	0.626 ± 0.005
6	1.82 ± 0.01	1.81 ± 0.01	0.633 ± 0.009	0.617 ± 0.009

TABLE III: The equal-time (ESS) and the integral-time dynamic multiscaling exponents for the fluid and the magnetic field from our simulations of decaying MHD turbulence for the magnetic Prandtl Number $\text{Pr}_M = 1.0$.

$[\langle \sum_n |u_n|^2 \rangle]^{1/2}$ and $b_{\text{rms}} = [\langle \sum_n |b_n|^2 \rangle]^{1/2}$. The Taylor microscale $\lambda \equiv \frac{\langle \sum_n (|u_n|^2/k_n^2) \rangle}{\langle \sum_n (|u_n|^2/k_n) \rangle}$, and the magnetic and fluid Reynolds-number, based on the Taylor microscale are, respectively, $\text{Re}_{\lambda,u} = u_{\text{rms}}\lambda/\nu$ and $\text{Re}_{\lambda,b} = b_{\text{rms}}\lambda/\eta$. Finally, we define the characteristic time scales for the fluid and the magnetic field via $\tau_u \equiv (u_{\text{rms}}k_1)^{-1}$ and $\tau_b \equiv (b_{\text{rms}}k_1)^{-1}$, respectively. The angular brackets in the above definitions imply an average over different initial configurations because we study decaying MHD turbulence in the remaining part of this paper.

V. RESULTS

We consider an unforced 3D MHD shell-model (with 22 shells) for 3D MHD with the initial shell-model velocities and magnetic fields $u_n = k_n^{-1/3} \exp(i\varphi_n)$ and $b_n = k_n^{-1/3} \exp(i\vartheta_n)$, with φ_n and ϑ_n random phases distributed uniformly on the interval $[0, 2\pi)$, respectively. We choose a time step $\delta t = 10^{-4}$. We obtain results for Pr_M equal to 0.1, 1.0, and 10.0. The various parameters of these simulations are given in Table I.

We calculate statistical quantities, like the energy spectrum, the equal-time structure functions, the time-dependent structure functions, and the various exponents extracted from them, only after the magnetic and fluid kinetic energy dissipation rates have reached their peaks. It is important to note that the peak in the dissipation

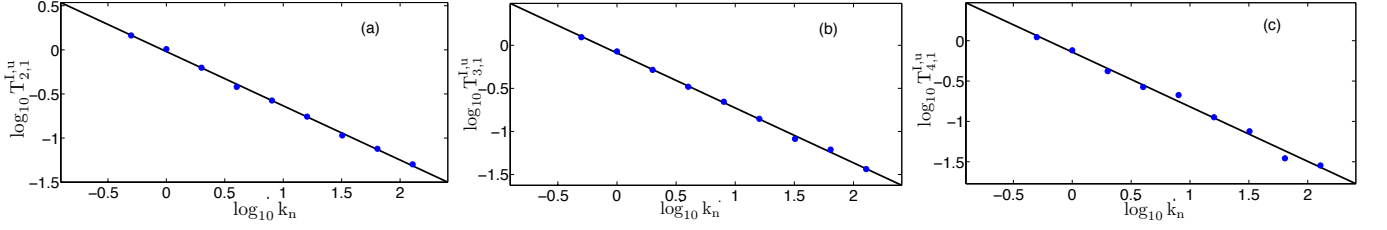


FIG. 3: (Color online) Log-log plots of the fluid integral-time scale $T_{p,1}^{I,u}$ versus the wave-vector for (a) $\text{Pr}_M = 0.1$ and $p = 2$, (b) $\text{Pr}_M = 1.0$ and $p = 3$, and (c) $\text{Pr}_M = 10.0$ and $p = 4$.

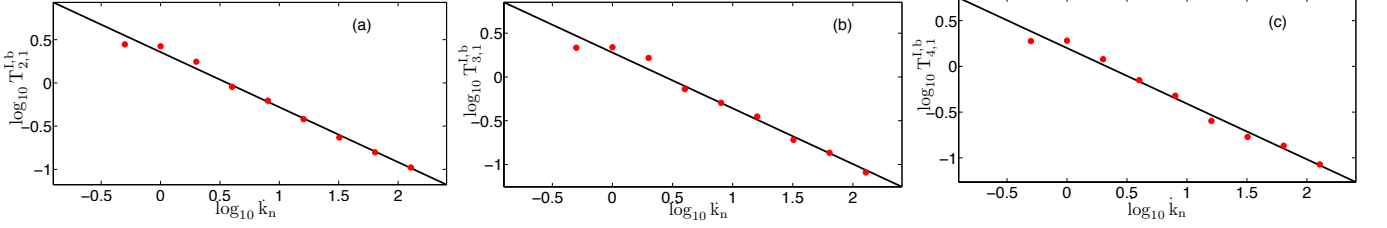


FIG. 4: (color online) Log-log plots of the fluid integral-time scale $T_{p,1}^{I,b}$ versus the wave-vector for (a) $\text{Pr}_M = 0.1$ and $p = 2$, (b) $\text{Pr}_M = 1.0$ and $p = 3$, and (c) $\text{Pr}_M = 10.0$ and $p = 4$.

p	ζ_p^u (ESS)	ζ_p^b (ESS)	$z_{p,1}^{I,u}$	$z_{p,1}^{I,b}$
1	0.356 ± 0.005	0.369 ± 0.005	0.653 ± 0.003	0.633 ± 0.002
2	0.690 ± 0.006	0.700 ± 0.006	0.673 ± 0.004	0.657 ± 0.002
3	1.0000	1.0000	0.679 ± 0.005	0.658 ± 0.004
4	1.284 ± 0.008	1.272 ± 0.008	0.687 ± 0.009	0.660 ± 0.006
5	1.543 ± 0.009	1.521 ± 0.009	0.70 ± 0.02	0.662 ± 0.009
6	1.79 ± 0.02	1.75 ± 0.03	0.70 ± 0.02	0.66 ± 0.01

TABLE IV: The equal-time (ESS) and the integral-time dynamic multiscaling exponents for the fluid and the magnetic field from simulations of decaying MHD turbulence for Prandtl Number $\text{Pr}_M = 10$.

rates, for both the fluid kinetic energy and the magnetic energy, occur at the same time here.

This time, at which the peak occurs, signals cascade completion, i.e., after this time, inertial-range fluid kinetic and the magnetic-energy spectra display K41 scaling with intermittency corrections. In Fig. (1) we show representative plots of the fluid and magnetic energy spectra for different values of Pr_M . We note that our spectral scaling exponents are compatible with the K41 result plus a small intermittency correction. The equal-time exponent-ratios, ζ_p^u/ζ_3^u and ζ_p^b/ζ_3^b , which we obtain by using the ESS procedure and from Eqs. (18), are shown in the insets of Fig. (1), for the three values of Pr_M used in our simulations; we list these ratios in Tables II, III, and IV; they are in agreement with previous studies (see, e.g., Ref. [1] and references therein).

We now turn our attention to the time-dependent structure functions (representative plots of which for the

magnetic field and different shell numbers for order-6 are shown in Fig. 2), whence we calculate the integral-time scales (cf. Eqs. (9-10) with $M = 1$)

$$T_{p,1}^{I,u}(k_n) = \int_0^{t_\mu} F_p^u(k_n, t) dt; \quad (21)$$

and

$$T_{p,1}^{I,b}(k_n) = \int_0^{t_\mu} F_p^b(k_n, t) dt; \quad (22)$$

we drop the index M for notational convenience; henceforth we use $M = 1$. In the above definitions, t_μ is the time at which $F_p^u(n, t) = \mu$ (or $F_p^b(n, t) = \mu$) with $0 \leq \mu \leq 1$. In principle we should use $\mu = 0$, i.e., $t_\mu = \infty$, but this is not possible in any numerical calculation because F_p^u and F_p^b cannot be obtained accurately for large t . We use $\mu = 0.7$; and we have checked in representative cases that our results do not change for $0.65 < \mu < 0.8$. Representative log-log plots of such integral-time scales are shown for various orders p and Pr_M for the fluid in Fig. (3) and for the magnetic field in Fig. (4). We see rather clean inertial-range scaling for both these quantities; and from numerical fits we obtain the dynamic multiscaling exponents $z_{p,1}^{I,u}$ and $z_{p,1}^{I,b}$. The values of all these exponents, and their dependence on Pr_M , are shown in Tables II, III, and IV. The mean values of these exponents are obtained from 50 different sets of statistically independent data; the mean of these is quoted as the exponent and their standard deviation as the error bar.

If we consider fluid turbulence alone, the analogs of these dynamic-multiscaling exponents satisfy linear bridge relations obtained in Ref. [6, 12, 13], which follow from a generalization [5, 6, 12, 13] of the multifractal

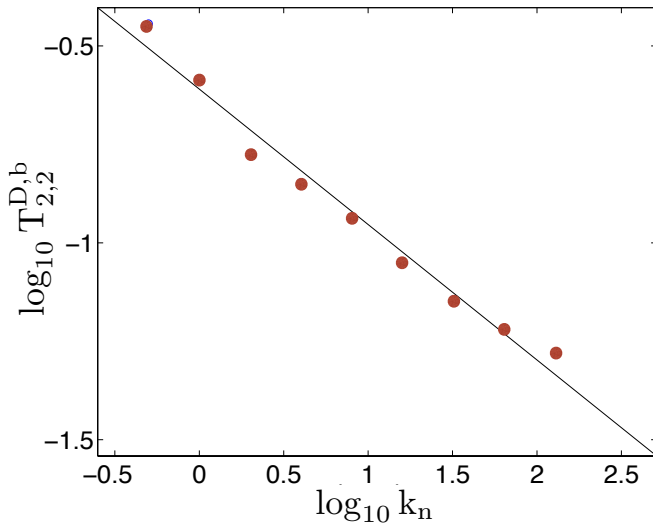


FIG. 5: (color online) Log-log plot of the magnetic derivative-time scale $T_{2,1}^{D,b}$ versus the wave-vector for $\text{Pr}_M = 1.0$. The thick black line indicates a slope of $z_{2,2}^{D,b} = 0.35$.

formalism [3] for turbulence. Unfortunately, this way of obtaining bridge relations cannot be generalized to the case of MHD turbulence: We must now deal with a joint multifractal distribution of both the velocity and the magnetic-field variables. To obtain the analogs of the fluid-turbulence bridge relations given above, additional decoupling approximations must be made for averages of products of powers of velocity and magnetic-field increments; such approximations have been used to obtain bridge relations for the case of passive-scalar turbulence [7, 13]. However, it is not possible to justify such additional decoupling approximations for the case of MHD turbulence because the magnetic field is actively advected by the fluid and, in turn, affects the advecting velocity field.

VI. CONCLUSIONS

Spatiotemporal correlation or structure functions are important measures by which we probe the statistical properties of turbulent flows, which arise from the dynamics and the coupling of the multiple spatial and temporal scales. We have developed the formalism for exploring the dynamic multiscaling of time-dependent structure functions that characterize MHD turbulence. Such dynamic multiscaling has been studied hitherto only for fluid and passive-scalar turbulence. Furthermore, we have carried out extensive numerical studies of such time-dependent structure functions in a shell model for 3D MHD turbulence [2] and thus shown that an infinity of dynamic-multiscaling exponents is required to characterize the multiscaling of time-dependent structure functions. Finally, we have demonstrated that these expo-

nents depend on the precise way in which time scales are extracted from these structure functions.

The measurement of two-point, spatiotemporal fluctuations, via time-dependent structure functions and their associated scaling exponents [14, 57, 58], is a challenging numerical task, especially if quasi-Lagrangian structure functions have to be obtained from direct numerical simulation (DNS) of hydrodynamical equations, as has been done for fluid turbulence in two and three dimensions [14, 57]. Given current computational resources, it is best to begin with shell-model studies, which have very special advantages compared to quasi-Lagrangian DNSs. Apart from the enormous range in Reynolds number that we can cover in shell models, the basic quasi-Lagrangian structure of shell models helps to eliminate trivial dynamic scaling, which arises because of the sweeping effect that we have discussed above.

Given recent advances in observational techniques for space plasmas and the solar winds [52], we expect that direct measurements of time-dependent structure functions should be possible in these systems. Our study of these structure functions in MHD turbulence is directly relevant to such experiments. It is important to realize the importance of such a calculation within the framework of shell models. For example, a recent shell-model study of Hall-MHD turbulence has provided an explanation of the spectral properties of turbulence in the solar wind [35].

Our numerical simulations of the MHD-shell-model equations are several orders of magnitude longer than those in earlier studies [2] and our Reynolds numbers are much higher than those achieved there. Given that the MHD system is considerably more complicated than its Navier-Stokes counterpart, it is not surprising that it is much harder to characterize dynamic multiscaling in the former than it is in the latter from *both theoretical and numerical points of view*. As we have mentioned above, we cannot obtain for MHD turbulence the analogs of bridge relations [6, 12, 13], which relate equal-time and dynamic-multiscaling exponents in fluid and passive-scalar turbulence. The exploration of dynamic multiscaling for the full MHD equations, via quasi-Lagrangian approaches [14, 57], remains a challenge.

In the case of previous shell-model studies of fluid and passive-scalar turbulence, it has been possible to extract, additionally the derivative-time-scale and the associated scaling exponents for the same [6, 7, 12, 13]. We find similar derivative time-scale exponents, defined via

$$T_{p,2}^{D,b}(k_n) = \left[\frac{1}{S_p^b(k_n)} \frac{\partial^2 \mathcal{F}_p^b(k_n, t)}{\partial t^2} \Big|_{t=0} \right]^{-1/2} \quad \text{and} \quad T_{p,2}^{D,u}(k_n) = \left[\frac{1}{S_p^u(k_n)} \frac{\partial^2 \mathcal{F}_p^u(k_n, t)}{\partial t^2} \Big|_{t=0} \right]^{-1/2},$$

for our MHD shell model. In

Fig. 5 we show a representative log-log plot of $T_{p,2}^{D,b}$ versus the wavenumber k_n to yield the scaling exponent $z_{p,2}^{D,b}$. We will, in future work, address systematically the issue of the derivative time-scale of different orders and explore the hierarchy of exponents for the integral and derivative

time-scales.

SSR and RP acknowledge the support of the Indo-French Center for Applied Mathematics (IFCAM); RP thanks the Department of Science and Technology, the Council of Scientific and Industrial Research (India) for support and SERC (IISc) for computational resources; and SSR thanks the AIRBUS Group Corporate Foun-

ation Chair in Mathematics of Complex Systems established in the ICTS as well as DST (India) project ECR/2015/000361 for support. GS acknowledges funding from the European Research Council under the European Union's Seventh Framework Programme, ERC Grant Agreement No 339032.

-
- [1] G. Sahoo, P. Perlekar, and R. Pandit, *New J. Phys.* **13**, 0130363 (2011).
 - [2] A. Basu, A. Sain, S.K. Dhar and R. Pandit, *Phys. Rev. Lett.* **81**, 2687 (1998).
 - [3] U. Frisch, *Turbulence: The Legacy of A.N. Kolmogorov* (Cambridge University, Cambridge, England, 1996).
 - [4] P. M. Chaikin and T. C. Lubensky, *Principles of Condensed Matter Physics* (Cambridge University, Cambridge, England, 2004).
 - [5] V. S. L'vov, E. Podivilov, and I. Procaccia, *Phys. Rev. E* **55**, 7030 (1997).
 - [6] D. Mitra and R. Pandit, *Phys. Rev. Lett.* **93**, 2 (2004).
 - [7] D. Mitra and R. Pandit, *Phys. Rev. Lett.* **95**, 144501 (2005).
 - [8] V.I. Belinicher and V.S. L'vov, *Sov. Phys. JETP* **66**, 303(1987).
 - [9] Y. Kaneda, T. Ishihara, and K. Gotoh, *Phys. Fluids* **11**, 2154 (1999).
 - [10] F. Hayot and C. Jayaprakash, *Phys. Rev. E* **57**, R4867 (1998).
 - [11] F. Hayot and C. Jayaprakash, *Int. J. Mod. Phys. B* **14**, 1781 (2000).
 - [12] R. Pandit, S.S. Ray, and D. Mitra, *Eur. Phys. J. B* **64**, 463 (2008).
 - [13] S.S. Ray, D. Mitra, and R. Pandit, *New J. Phys.* **10**, 033003 (2008).
 - [14] S.S. Ray, D. Mitra, P. Perlekar, and R. Pandit, *Phys. Rev. Lett.* **107**, 184503 (2011).
 - [15] A.M. Obukhov, *Atmos. Oceanic Phys.* **10**, 127 (1974).
 - [16] V.N. Desnyansky and E.A. Novikov, *Prikl. Mat. Mekh.* **38**, 507 (1974).
 - [17] E.B. Gledzer, *Sov. Phys. Dokl. SSSR* **18**, 216 (1973).
 - [18] K. Ohkitani and M. Yamada, *Prog. Theor. Phys.* **81**, 32941 (1982).
 - [19] M.H. Jensen, G. Paladin, and A. Vulpiani, *Phys. Rev. A* **43**, 798 (1991).
 - [20] D. Pisarenko, L. Biferale, D. Courvoisier, U. Frisch, and M. Vergassola, *Phys. Fluids A* **5**, 2533 (1993).
 - [21] S.K. Dhar, A. Sain, A. Pande, and R. Pandit, *Pramana J. Phys.: Special Issue on Nonlinearity and Chaos in the Physical Sciences* **48**, 325 (1997).
 - [22] S.K. Dhar, A. Sain, and R. Pandit, *Phys. Rev. Lett.* **78**, 2964 (1997).
 - [23] L. Biferale, *Annu. Rev. Fluid Mech.* **35**, 441 (2003).
 - [24] T. Bohr, M.H. Jensen, G. Paladin, and A. Vulpiani, *Dynamical systems approach to turbulence*, Cambridge Nonlinear Science Series (Cambridge University Press, UK, 2005).
 - [25] P.D. Ditlevsen, *Turbulence and shell models* (Cambridge University Press, UK, 2010).
 - [26] V.S. Lvov, E. Podivilov, A. Pomyalov, I. Procaccia, and D. Vandembroucq, *Phys. Rev. E* **58**, 1811 (1998).
 - [27] C. Kalelkar and R. Pandit, *Phys. Rev. E* **69**, 046304 (2004).
 - [28] G. Sahoo, D. Mitra, and R. Pandit, *Phys. Rev. E* **81**, 036317 (2010).
 - [29] P. Frick and D. Sokoloff, *Phys. Rev. E* **57**, 4155 (1998).
 - [30] A. Brandenburg, K. Enqvist, and P. Olesen, *Phys. Rev. D* **54**, 1291 (1996).
 - [31] P. Giuliani and V. Carbone, *Europhys. Lett.* **43**, 527 (1998).
 - [32] D. Hori, M. Furukawa, S. Ohsaki, and Z. Yoshida, *J. Plasma Fusion Res.* **81**, 141 (2005).
 - [33] D. Hori and H. Miura, *J. Plasma Fusion Res.* **3**, S1053 (2008).
 - [34] S. Galtier, *Phys. Rev. E* **77**, 015302 (2008).
 - [35] D. Banerjee, S.S. Ray, G. Sahoo, and R. Pandit, *Phys. Rev. Lett.* **111**, 174501 (2013).
 - [36] C. Kalelkar, R. Govindarajan, and R. Pandit, *Phys. Rev. E* **72**, 017301 (2005); S.S. Ray and D. Vincenzi, *arXiv:1603.01692v1*, (2016).
 - [37] E. Aurell, G. Boffetta, A. Crisanti, P. Frick, G. Paladin, and A. Vulpiani, *Phys. Rev. E* **50**, 4705 (1994).
 - [38] P. Giuliani, M.H. Jensen, and V. Yakhot, *Phys. Rev. E* **65**, 036305 (2002).
 - [39] Y. Hattori, R. Rubinstein, and A. Ishizawa, *Phys. Rev. E* **70**, 046311 (2004).
 - [40] S.S. Ray and A. Basu, *Phys. Rev. E* **84**, 036316 (2011).
 - [41] D.H. Wacks and C.F. Barenghi, *Phys. Rev. B* **84**, 184505 (2011).
 - [42] L. Boué, V. Lvov, A. Pomyalov, and I. Procaccia, *Phys. Rev. B* **85**, 104502 (2012).
 - [43] L. Bou, V. Lvov, A. Pomyalov, and I. Procaccia, *Phys. Rev. Lett.* **110**, 014502 (2013).
 - [44] V. Shukla and R. Pandit, *arXiv:1508.00448v2* (2015).
 - [45] D. Biskamp, *Magnetohydrodynamical Turbulence*, (Cambridge University Press, Cambridge, England, 2003); M.K. Verma, *Phys. Rep.*, **401**, 229 (2004).
 - [46] P.D. Mininni and A. Pouquet, *Phys. Rev. E* **80**, 025401 (2009).
 - [47] A.N. Kolmogorov, *Dokl. Akad. Nauk. SSSR* **30**, 9 (1941); **30** 301 (1941); **31**, 538 (1941); **32**, 16 (1941); *Proc. R. Soc. London, Ser. A* **434**, 9 (1991); **434**, 15 (1991); *C.R. Acad. Sci. USSR* **30**, 301 (1941).
 - [48] P.S. Iroshnikov, *Sov. Astron.* **7**, 566 (1964).
 - [49] R.H. Kraichnan, *Phys. Fluids* **8**, 1385 (1965).
 - [50] M. Dobrowlny, A. Mangeney, and P. Veltri, *Phys. Rev. Lett.*, **45**, 144 (1980).
 - [51] S. Galtier, A. Pouquet, and A. Mangeney, *Phys. Plasmas* **12**, 092310 (2005); <http://dx.doi.org/10.1063/1.2052507>.
 - [52] R. Marino *et al.*, *Planetary & Space Science* **59**, 592-597 (2011); *Astrophys. J.* **750**, 41, (2012).
 - [53] S.B. Pope, *Turbulent Flows* (Cambridge University, Cambridge, UK, 2000).

- [54] V.S. L’vov and V.L. Lebedev, Phys. Rev. E **47**, 1794 (1993).
- [55] L.P. Kadanoff, D. Lohse, J. Wang, and R. Benzi, Phys. Fluids **7**, 617 (1995).
- [56] R. Benzi, S. Ciliberto, C. Baudet, F. Massaioli and S. Succi, Phys. Rev. E **48**, R29 (1993); S. Chakraborty, U. Frisch and S.S. Ray, *J. Fluid Mech.* **649**, 275 (2010).
- [57] L. Biferale, E. Calzavarini, and F. Toschi, Phys. Fluids **23**, 085107 (2011).
- [58] G. He, G. Jin and Y. Yang, Annu. Rev. Fluid Mech. **49**, 51-71 (2017).